Case Studies in Thermal Engineering 36 (2022) 102193

Contents lists available at ScienceDirect

Case Studies in Thermal Engineering

journal homepage: www.elsevier.com/locate/csite

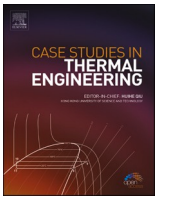

# Surface tension of esters. Temperature dependence of the influence parameter in density gradient theory with Peng-Robinson equation of state

Isidro Cachadiña [a,*], Ariel Hernández [a,b], Ángel Mulero [a,**]

[a] Departamento de Física Aplicada, Universidad de Extremadura, Spain
[b] Departamento de Ingeniería Industrial, Facultad de Ingeniería, Universidad Católica de la Santísima Concepción, Alonso de Ribera 2850, Concepción, Chile

ARTICLE INFO

*Keywords:*
Surface tension
Peng-Robinson equation of state
Gradient density theory
Influence parameter
Esters

ABSTRACT

A new temperature-dependent correlation for the reduced influence parameter of the density gradient theory, when used with the Peng-Robinson equation of state, is proposed and compared with other correlations found in the literature. The proposed correlation is linear in its two fitting parameters and contains a universal exponent related to the one from the liquid-vapor phase transition universal scale law. The overall absolute deviation (OAAD) respect 1275 surface tension data for 39 esters is 1.37%. Only the proposal from Zuo and Stenby with OAAD = 1.29%, yields similar results with the same number of parameters.

Fitting parameters for the new correlation proposed and those from Zuo and Stenby are given for the fluids considered in this work.

## 1. Introduction

Esters and their mixtures are commonly used in different industrial processes in which their surface tension, together with the density and viscosity, are important properties to be taken into account. We can mention some uses as low volatility solvents for inks, polymers, resin, and many other applications [1–3].

Several methods as the parachor [4], the corresponding-states principle [5], and the density functional theory [6] have been used to correlate or predict the dependence of fluids surface tension with temperature, being the Density Gradient Theory (DGT) very successful in this purpose [7–14]. This theory was developed by Cahn and Hilliard [15], and the method based on the combination of DGT and an equation of state (EoS) was proposed by Carey et al. [8]. In the DGT, the Helmholtz energy of the interphase is obtained as a sum of two terms: a uniform one corresponding to the homogeneous system and another one proportional to the square of the density gradient. The surface tension can then be defined in terms of the integral of the square of the density gradient and obtained by knowing the values of the saturated vapor and liquid densities, the saturation pressure, and an analytical expression for the Helmholtz energy density [8,16]. All these properties can be obtained from an EoS.

Following this DGT + EoS method, the surface tension $\sigma$ at temperature $T$ is calculated as [8,16]:

* Corresponding author.
** Corresponding author.
*E-mail addresses:* icacha@unex.es (I. Cachadiña), mulero@unex.es (Á. Mulero).

https://doi.org/10.1016/j.csite.2022.102193
Received 2 March 2022; Received in revised form 20 May 2022; Accepted 5 June 2022
Available online 23 June 2022

$$\sigma = \int_{\rho_V^0}^{\rho_L^0} \sqrt{2c\left[f_0 - \rho\left(\frac{\partial f_0}{\partial \rho}\right)_T^0 + p^0\right]}\, d\rho, \tag{1}$$

where $\rho$ is the density, and $p^0$, $\rho_V^0$, and $\rho_L^0$ are the saturation pressure, vapor and liquid densities at temperature $T$, respectively (the superscript $^0$ indicates saturation properties). The parameter $c$ is the so-called influence parameter, and $f_0$ is the Helmholtz energy density given by:

$$f_0(\rho, T) = \rho f(\rho, T), \tag{2}$$

where $f(\rho, T)$ is the Helmholtz energy of the system.

From a pressure-based EoS the associated Helmholtz energy is determined by considering that it can be split into an ideal ($f^\circ$) and a residual ($f^r$) contribution [17], as

$$f(\rho, T) = f^r(\rho, T) + f^\circ(\rho, T). \tag{3}$$

The residual part is obtained from the pressure EoS as:

$$f^r(\rho, T) = \int \frac{p}{\rho^2} d\rho - RT\log \rho, \tag{4}$$

where $p$ is the pressure, while the ideal contribution $f^\circ$ is obtained from the ideal isobaric caloric capacity $c_p^\circ(T)$ as:

$$f^\circ(\rho, T) = h_0 - Ts_0 - RT + RT\ln\frac{T}{T_0} + RT\ln\frac{\rho}{\rho_0} + \int_{T_0}^{T} c_p^\circ(T) dT - T\int_{T_0}^{T} \frac{c_p^\circ(T)}{T} dT. \tag{5}$$

Here, $h_0$ and $s_0$ are the ideal enthalpy and entropy of the reference state at $T_0$ and $\rho_0$, so that:

$$h^\circ(T_0) = h_0, \qquad s^\circ(\rho_0, T_0) = s_0.$$

It must be noted that the value of $c_p^\circ(T)$ considered for the ideal gas contribution has no influence in Eq. (1) since the integration is done at constant temperature (see the Appendix).

The DGT + EoS method presents some advantages when compared with others:

i) It is theoretically sound, as the fundamentals of the van der Waals theory are applied. The system inhomogeneities are given as a function of the gradient density and can be expressed as a function of the direct correlation function [15,18].
ii) The coexistence densities at the vapor-liquid equilibrium and the saturation pressure are obtained directly from the EoS, so other data sources, or analytical expressions, are not needed.
iii) It permits the calculation of the surface or interfacial tension, the density profiles and their thickness, the surface enthalpy and entropy, and some other relevant properties for the adsorption processes [11].

On the other hand, the DGT + EoS method has certain limitations. According to Liang et al. [19], the method is not entirely general, as a fitting procedure is needed to obtain the influence parameter. This fact has the disadvantage that the values obtained, or the correlations proposed, are not always transferable to other substances or other temperature ranges [16,20]. Finally, the required calculations are not always straightforward and must be made carefully to avoid wrong results.

Besides, when applying the DGT + EoS, it has to be noted that: i) The influence parameter will depend on the EoS used; ii) EoS does not pay much attention to the behavior in the region between the liquid and vapor densities, being this region taken into consideration in the Maxwell construction that leads to the equal-area equilibrium condition; and iii) The argument of the square root in (1) must be positive: an accurate EoS with multiple van der Waals loops could lead to a negative argument, and the method could be not applicable.

Despite these limitations, the mentioned advantages are valuable, and the DGT + EoS method has been widely used with accurate results for both pure fluids and mixtures, considering different analytical expressions for the EoS and the influence parameter [7–10, 16,19–31].

Since Carey et al. [8] applied for the first time the DGT + EoS in 1978, according to Garrido et al., more than 150 scientific papers related to the gradient theory have been published up to 2016 [16], and today the number has been greatly increased. The most used equations have been the PR EoS and Statistical-Associating-Fluid-Theory (SAFT) variations. On the other hand, Chow et al. [21], and Larsen et al. [23], reported that Soave-Redlich-Kwong (SRK) and Cubic-Plus-Association (CPA) were other widely used equations of state.

Although it is well-known that cubic EoS give poor results in the prediction of liquid densities [32,33], they are still used because of their good balance between simplicity and predictive capability. Moreover, cubic EoS are reliable and allow the direct incorporation of the critical properties [32,34], are suitable for quick calculations, and apply to a wide range of temperature and pressure, giving a satisfactory result for vapor-liquid equilibria (VLE) at low and high pressure.

The good results yielded in the prediction of surface tension with the combination of cubic EoS and DGT [8–11,22,23,26,27,35–37] are explained because influence parameter compensates the deviations between the experimental liquid saturation densities and the predicted by cubic EoS.

## 2. Temperature dependence of the influence parameter

The aim of this work is to explore the temperature dependency of the influence parameter when using the Peng-Robinson cubic EoS (PR-EoS) [38] together with the DGT. (As the PR-EoS has been the subject of many modifications since first published, we address the reader to the paper from López-Echeverry et al. [39] where many of these modifications are compiled).

The analytical expression of the classical PR-EoS is:

$$p = \frac{RT}{v-b} - \frac{a}{(v+b)^2 - 2b^2} \tag{6}$$

where $v = \rho^{-1}$ the molar volume, $R$ the ideal gas constant, $a$ is the cohesive parameter, and $b$ is the covolume parameter. The values of $a$ and $b$ are calculated from the fluid critical temperature $T_c$, critical pressure $p_c$, and acentric factor $\omega$ as [38]:

$$a = 0.45724 \frac{(RT_c)^2}{p_c} \alpha(T) \tag{7}$$

$$\alpha(T) = \left[1 + (0.37464 + 1.54226\ \omega - 0.26992\ \omega^2)\left(1 - \sqrt{\frac{T}{T_c}}\right)\right]^2 \tag{8}$$

$$b = 0.07780 \frac{RT_c}{p_c} \tag{9}$$

where $\alpha(T)$ is the thermal cohesion function.

As said before, the influence parameter $c(T_i)$ at temperature $T_i$ needs to be determined from the corresponding surface tension datum $\sigma_i$ as:

$$c(T_i) = \frac{\sigma_i^2}{I}, \tag{10}$$

with

$$I = \left\{ \int_{\rho_V^0}^{\rho_L^0} \sqrt{2\left[f_0 - \rho\left(\frac{\partial f_0}{\partial \rho}\right)_T^0 + p^0\right]}\, d\rho \right\}^2, \tag{11}$$

where the superindex $^0$ indicates saturation properties. The saturation pressure ($p^0$), vapor density ($\rho_V^0$), and liquid density ($\rho_L^0$) at the considered temperature, $T_i$ are determined by solving the vapor-liquid equilibrium conditions:

$$p(T_i, \rho_L^0) = p(T_i, \rho_V^0) = p^0 \tag{12}$$

and

$$0 = \int_{\rho_V^0}^{\rho_L^0} \frac{p(T_i, \rho) - p^0}{\rho^2} d\rho. \tag{13}$$

We have checked that, in the case of high acentric factor values and low temperatures, double-precision floats (about 16 decimal digits) are not enough to solve the system of Eqs. (12) and (13), and yield the values of $\rho_V^0$, $\rho_L^0$, and $p^0$ with the appropriate accuracy to be used as inputs in (11). Thus, our computer program uses quadruple precision (33 decimal digits approx.) in all the intermediate calculations, to determine $p^0$, $\rho_V^0$, and $\rho_L^0$ with at least 20 exact significant figures.

The integral in (11) is evaluated numerically using the Romberg integration with Richardson's deferred approach to the limit [40]. The number of significant figures for this value is set to 10 to retain enough accuracy in further calculations.

In the study and proposal of correlations for the influence parameter, it is usual to write the reduced influence parameter ($c^*$), defined as [7,9,10,41]:

$$c^* = \frac{c}{a b^{2/3}}, \tag{14}$$

where $a$ and $b$ are defined in (7) and (9), and $c^*$ is given in mol$^{2/3}$.

Several authors have studied the temperature dependence of the reduced influence parameter. Thus, Cornelisse [41] found that a constant value for the reduced influence parameter cannot be applied successfully in the range $0.3 < T_r < 0.85$, with $T_r = T/T_c$, while Miqueu et al. [10] proposed that

$$c^* = m_0 + m_1 \tau, \tag{15}$$

can be applied in the range $0.02 < \tau < 0.71$ or $0.29 < T_r < 0.98$, being

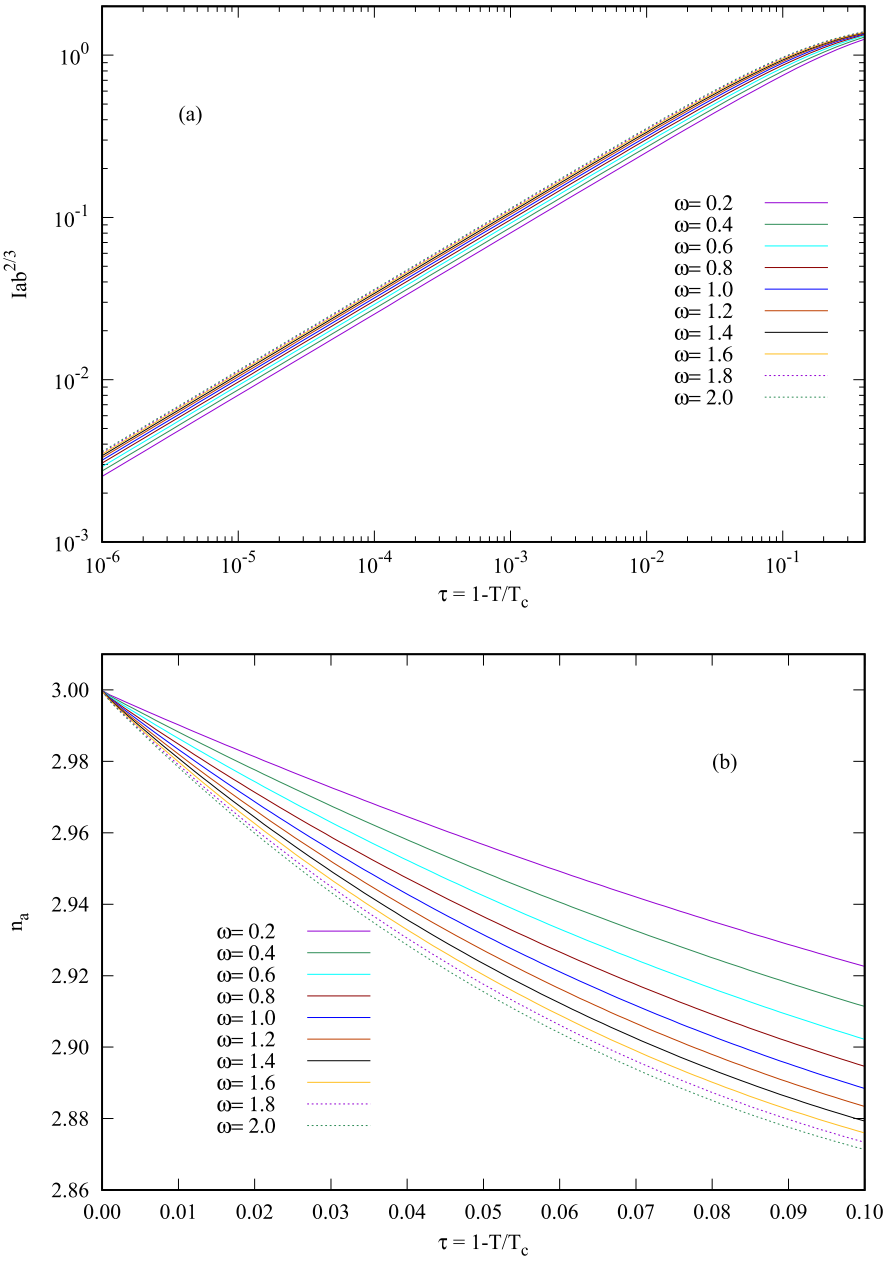


**Fig. 1.** (a) log-log representation of $Iab^{2/3}$ vs $\tau$ for different acentric factors ranging from 0.2 to 2.0. (b) Slope of the curves in (a) evaluated with Eq. (23).

$$\tau = 1 - \frac{T}{T_c}.$$

Oliveira et al. [7] proposed a quadratic polynomial:

$$c^* = m_0 + m_1\tau + m_2\tau^2, \tag{16}$$

that was successfully applied to esters in the range $0.45 < T_r < 0.85$, i.e., far from the triple and critical points. Also, the observation of the asymptotic behavior for $\tau \to 0$ lead to Zuo and Stenby [9] to the proposal:

$$c^* = m_0\tau^n, \tag{17}$$

that has the analytical form of a power law, where the parameters $m_0$ and $n$ are determined for each fluid, being $n$ in the range $-0.4$ to

−0.6 for hydrocarbons [9].

Taking into account that the surface tension ($\sigma$) and $I$ are zero at the critical point, the power law of the reduced influence parameter must balance the different power laws followed by $\sigma$ and $I$. Thus, the combination of Eqs. (10) and (14):

$$c^* = \frac{\sigma^2}{Iab^{2/3}}, \tag{18}$$

can be used to relate the different power laws followed by $c^*$, $\sigma$, and $Iab^{2/3}$. Thus, assuming that:

$$c^*(\tau \to 0) \propto \tau^{n_c}, \tag{19}$$

$$\sigma(\tau \to 0) \propto \tau^{n_\sigma}, \tag{20}$$

and

$$Iab^{2/3}(\tau \to 0) \propto \tau^{n_a}, \tag{21}$$

the following relation between the exponents is obtained:

$$n_c = 2n_\sigma - n_a. \tag{22}$$

The value of $n_a$ depends only on the EoS used, and it is determined as the slope of the curve $\log(Iab^{2/3})$ vs. $\log \tau$. Fig. 1a shows the different log-log curves obtained by using the PR EoS when considering several acentric factors for temperatures very close to the critical one. In the range $\tau < 10^{-2}$, the curves are parallel lines where the corresponding exponents ($n_a$), obtained numerically as:

$$n_a = \left. \frac{d\log\left(Iab^{2/3}\right)}{d\log \tau} \right|_\tau, \tag{23}$$

approaches to $n_a = 3$ when $\tau \to 0$ (see Fig. 1b), regardless the acentric factor considered.

Once this value have been determined, we have that:

$$n_c = 2n_\sigma - 3,$$

and the reduced influence parameter will show an asymptote if $n_\sigma < 1.5$.

In the estimation of $n_\sigma$, it is essential to point out the difficulty of obtaining surface tension values near the critical point. In general, when some data are available, they have very high experimental uncertainties, and it is common to find two or more data trends when considering more than one experimental source [42–47]. Due to this lack of experimental data, one can find datasets being predicted using Sugden's method [4], which is based on the experimental evidence that the surface tension can be correlated with the difference between liquid and vapor coexistence densities as

$$\sigma(T) = \mathcal{P}^4(\rho_L^0 - \rho_V^0)^4, \tag{24}$$

where $\mathcal{P}$ is the parachor. This parameter ($\mathcal{P}$) can be obtained by a fit to the experimental surface tension, or by a group contribution estimation [48,49].

Our hypothesis here is to consider that the relation given in Eq. (24) is valid near the critical point, and that the liquid-vapor phase transition follows the three dimensional Ising universality class [50,51]:

$$(\rho_L^0 - \rho_V^0) \propto \tau^\beta, \tag{25}$$

with $\beta \simeq 0.326$, the critical exponent. The insertion of (25) in (24) leads to the universal exponent $n_\sigma = 4\beta = 1.304$, and according to Eq. (22), to:

$$n_c = 8\beta - 3 = -0.392. \tag{26}$$

This value is close to the ones reported by Zuo and Stenby for hydrocarbons [9], that are in the range −0.4 to −0.6.

The correlation proposed in this work contains the mentioned exponent and two fluid-dependent parameters $m_0$ and $m_1$ as:

$$c^* = m_0(t^{-0.392} - 1) + m_1, \tag{27}$$

where $t$ is defined as

$$t = (T_c - T)/(T_c - T_t), \tag{28}$$

where $T_t$ is the triple point temperature. Thus, the variable $t$ ranges from 0 (critical point temperature) to 1 (triple point temperature), being $c^*(1) = m_1$. It has to be noted that Eqs. (15)–(17) can be used in terms of $t$, since $t$ and $\tau$ are proportional ($t = \tau[1 - T_t/T_c]$).

In the next sections, the behavior of the correlations given by Eqs. (15)-(17) and (27) for a selection of esters will be studied and compared. The hypothesis of the existence of an universal exponent related to the density critical exponent, Eq. (27), will be evaluated.

**Table 1**
List of the fluids considered in this work (in alphabetic order), number of data considered ($N_{fluid}$), temperature range and data source references.

| Index | Name | $N_{fluid}$ | Range $T$ (K) | Range $T_r$ | Data Source Refs. |
|---|---|---|---|---|---|
| 1 | 2,2,4-trimethyl-1,3-pentanediol diisobutyrate | 17 | 203.15 – 674.84 | 0.288 - 0.956 | [52] |
| 2 | 2-ethoxyethyl acetate | 20 | 211.45 – 546.57 | 0.348 - 0.900 | [52,53,59] |
| 3 | 2-ethylhexyl acrylate | 13 | 183.15 – 583.15 | 0.280 - 0.890 | [52] |
| 4 | di(2-ethylhexyl) terephthalate | 18 | 225.15 – 731.16 | 0.277 - 0.900 | [52,54] |
| 5 | di-n-butyl phthalate | 19 | 238.15 – 765.51 | 0.299 - 0.960 | [52–54,60] |
| 6 | dibutyl terephthalate | 18 | 293.15 – 756.95 | 0.372 - 0.962 | [52] |
| 7 | diethyl phthalate | 41 | 283.15 – 698.40 | 0.365 - 0.900 | [52–54,59–62] |
| 8 | diethylene glycol monobutyl ether acetate | 13 | 240.95 – 611.10 | 0.355 - 0.900 | [52,63] |
| 9 | dimethyl maleate | 30 | 254.15 – 604.15 | 0.377 - 0.895 | [52–54,59,60] |
| 10 | ethyl acetate | 142 | 199.15 – 518.15 | 0.381 - 0.990 | [4,52–54,56,59,60,64–72] |
| 11 | ethyl acrylate | 48 | 201.95 – 491.95 | 0.365 - 0.890 | [52,60,73] |
| 12 | ethyl caprate | 30 | 253.20 – 655.27 | 0.368 - 0.952 | [52,53,60,74–76] |
| 13 | ethyl caprylate | 55 | 229.00 – 616.92 | 0.353 - 0.951 | [52,53,59,67,74–77] |
| 14 | ethyl laurate | 30 | 283.15 – 684.03 | 0.395 - 0.955 | [52,53,60,66,74–76] |
| 15 | ethyl myristate | 27 | 293.15 – 708.66 | 0.397 - 0.959 | [52,53,60,75,76] |
| 16 | ethyl oleate | 20 | 253.67 – 694.89 | 0.329 - 0.900 | [52,54,74,75] |
| 17 | ethyl palmitate | 36 | 298.15 – 728.47 | 0.393 - 0.959 | [52–54] |
| 18 | ethyl phenyl acetate | 35 | 243.75 – 631.89 | 0.347 - 0.900 | [52–54,60] |
| 19 | ethyl stearate | 20 | 305.65 – 700.11 | 0.393 - 0.900 | [52–54] |
| 20 | isopentyl butyrate | 31 | 189.00 – 556.95 | 0.305 - 0.900 | [52–54,60,66] |
| 21 | methyl caprylate | 51 | 236.20 – 618.46 | 0.363 - 0.950 | [31,52,53,58–60,67,74,76,78–80] |
| 22 | methyl erucate | 18 | 271.95 – 725.58 | 0.337 - 0.900 | [52,58,74] |
| 23 | methyl formate | 64 | 203.15 – 483.15 | 0.417 - 0.992 | [4,52–54,59,60,64,70,81–83] |
| 24 | methyl linoleate | 23 | 233.93 – 690.66 | 0.305 - 0.900 | [52,58] |
| 25 | methyl linolenate | 18 | 216.15 – 692.46 | 0.281 - 0.900 | [52,58,74] |
| 26 | methyl methacrylate | 13 | 224.95 – 504.95 | 0.397 - 0.892 | [52,60] |
| 27 | methyl myristate | 42 | 291.85 – 667.08 | 0.394 - 0.900 | [31,52,53,58,59,74,76,78,79,84] |
| 28 | methyl oleate | 31 | 253.65 – 699.30 | 0.326 - 0.900 | [52,54,58,60,85,86] |
| 29 | methyl palmitate | 32 | 303.05 – 685.98 | 0.398 - 0.900 | [31,52,53,58,59,74,84] |
| 30 | methyl stearate | 38 | 312.15 – 702.99 | 0.400 - 0.900 | [31,52–54,58,74,79,84–86] |
| 31 | n-butyl acrylate | 36 | 208.55 – 528.55 | 0.349 - 0.884 | [52,73] |
| 32 | *tert*-butyl methacrylate | 15 | 225.15 – 529.47 | 0.383 - 0.900 | [52] |
| 33 | tricaprin | 46 | 308.55 – 845.81 | 0.352 - 0.965 | [52–54,75,87] |
| 34 | tricaprylin | 59 | 293.15 – 820.23 | 0.345 - 0.964 | [52–54,59,75,88–91] |
| 35 | trilaurin | 20 | 333.15 – 866.41 | 0.372 - 0.966 | [52–54,87] |
| 36 | trimyristin | 14 | 333.15 – 821.16 | 0.365 - 0.900 | [52,87] |
| 37 | tripalmitin | 40 | 339.05 – 893.72 | 0.366 - 0.966 | [52–54,87] |
| 38 | tristearin | 34 | 353.15 – 905.93 | 0.377 - 0.968 | [52–54,87] |
| 39 | vinyl acetate | 18 | 180.35 – 460.35 | 0.347 - 0.887 | [52,54,56,59,60] |

## 3. Sources of data

Surface tension data of esters (including experimental, smoothed and estimated ones) have been compiled from DIPPR [52] and DETHERM [53] databases, the books of Wohlfarth and Wohlfarth [54–56], and a great number of bibliographic references (see Table 1 and Refs. [46,47] for details).

Once the surface tension data have been processed and screened [46,47], the fluids with the following two conditions were selected: 1) The percentage of data points selected, generated with the predictive Sugden [57] method, must be below 90%. 2) The available data must cover more than 80% of the temperature range between the triple and critical point temperatures.

Forty fluids fulfill these requisites, but the data from trioctyl trimellitate were not taken into consideration because of the different tendencies followed by some datasets from different sources [47]. Finally, 39 fluids with 1275 values for the surface tension have been taken into account in this study. Names of these esters, the number of data selected, the temperature range considered, and the sources used for the data are shown in Table 1.

The values of the parameters required to determine the cubic EoS properties, such as critical pressure ($p_c$), critical temperature ($T_c$), and acentric factor ($\omega$), besides the triple point temperature ($T_t$), have been obtained from the DIPPR database [52].

## 4. Fitting procedure and statistics

Powell's minimization method [40] was used to obtain all the correlation parameters for each fluid. The function minimized was the absolute average deviation (AAD) of the surface tension data, defined as:

$$\mathrm{AAD} = \frac{1}{N_{fluid}} \sum_{i=1}^{N_{fluid}} |PD_i|, \tag{29}$$

where $N_{fluid}$ is the number of available data for each fluid, and $\mathrm{PD}_i$ is the percentage deviation of the datum ($T_i$, $\sigma_i$) respect the calculated one $\sigma_{calc}(T_i)$:

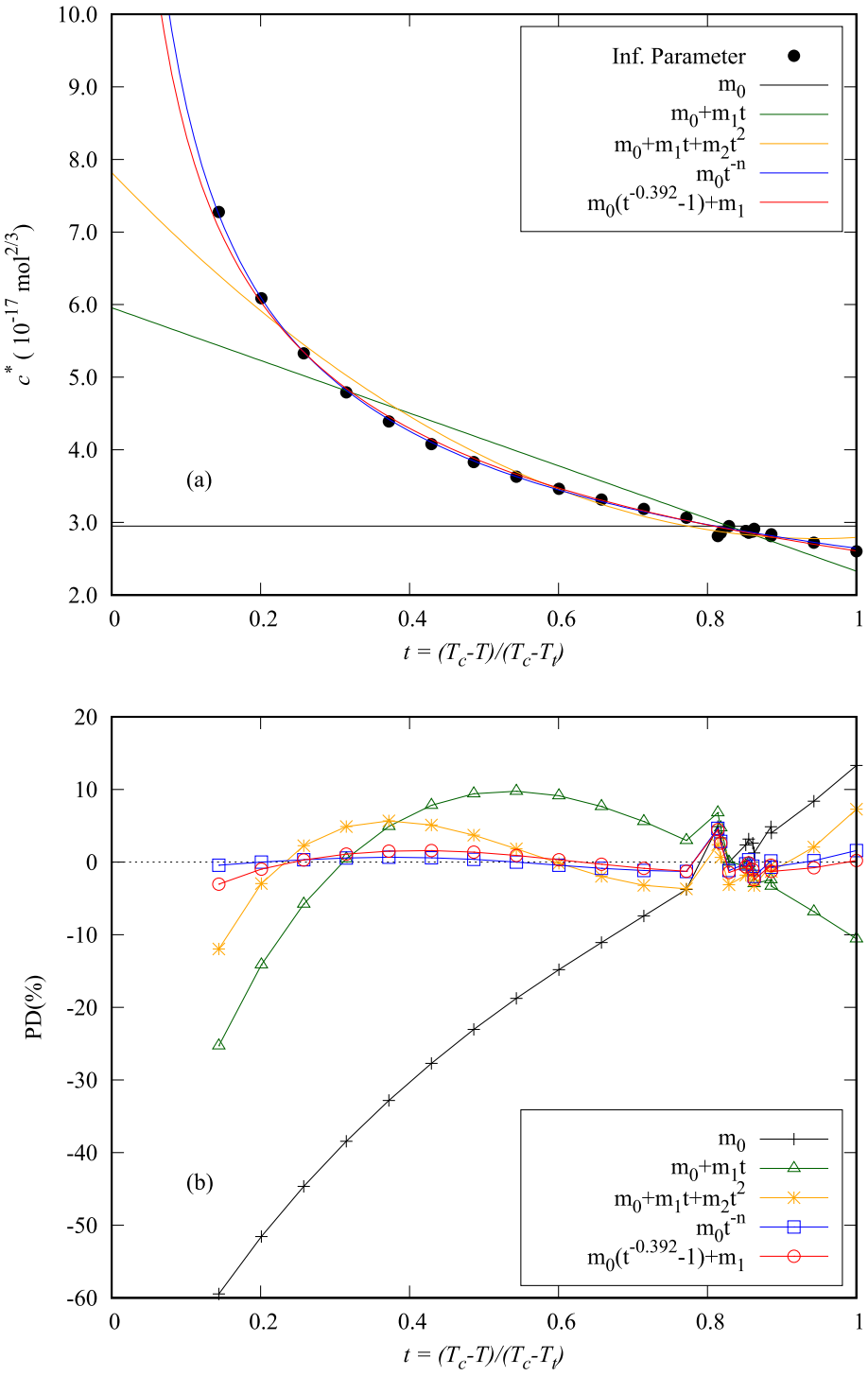


**Fig. 2.** (a) Reduced influence parameter for methyl linoleate obtained with Eq. (10) (points) and predicted influence parameter curves when the different proposals are considered (lines). (b) Relative percentage deviations of the influence parameter respect all the correlations considered.

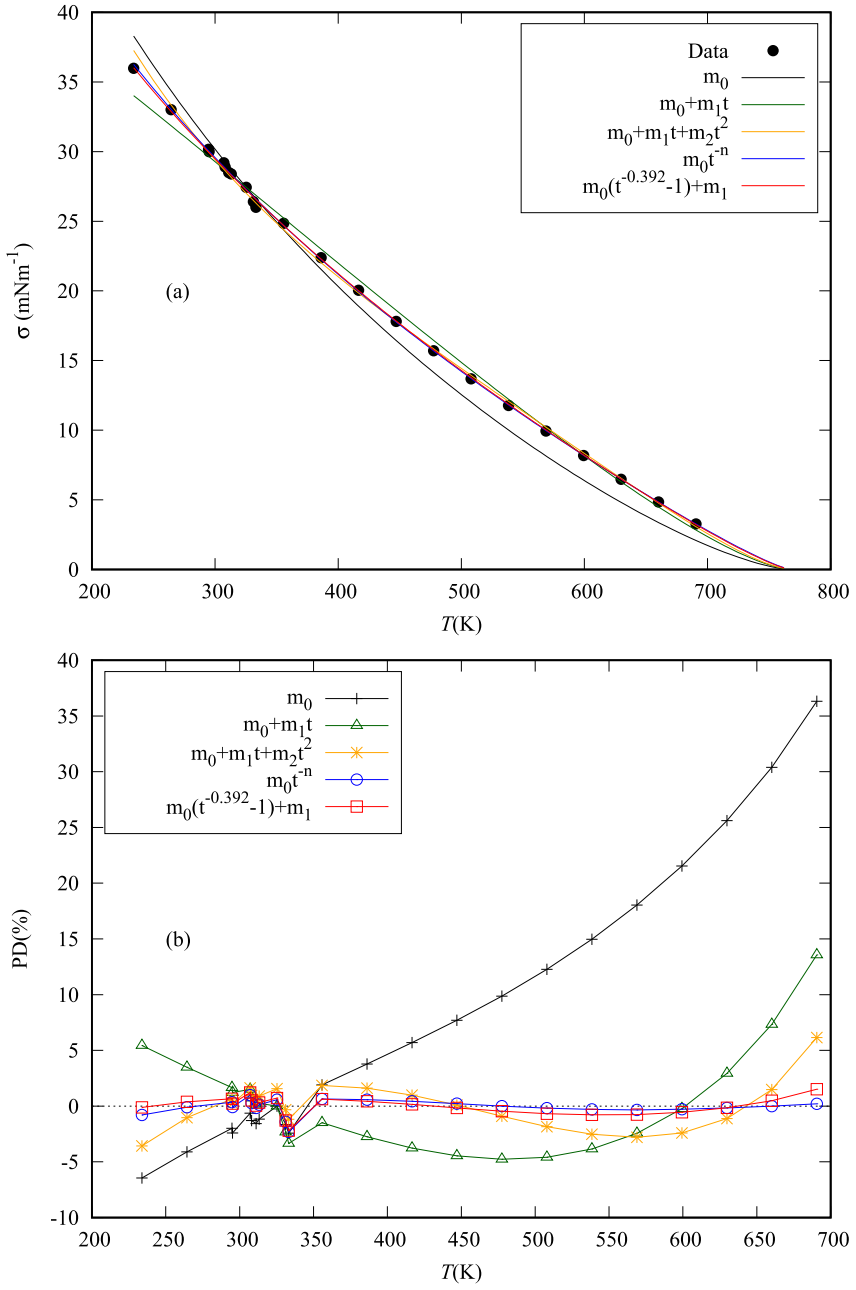


**Fig. 3.** Surface tension and $PD_i$ values obtained for methyl linoleate when the different correlations for the reduced influence parameter are considered.

$$PD_i = 100 \cdot \frac{\sigma_{calc}(T_i) - \sigma_i}{\sigma_i}. \tag{30}$$

Besides the AAD, the comparison between the different proposals is done attending the following statistical figures: maximum absolute percentage deviation:

$$PD_{max} = \max|PD_i| \qquad (i = 1, \ldots, N_{fluid}), \tag{31}$$

mean deviation (MD)

$$MD = \frac{1}{N_{fluid}} \sum_{i=1}^{N_{fluid}} PD_i, \tag{32}$$

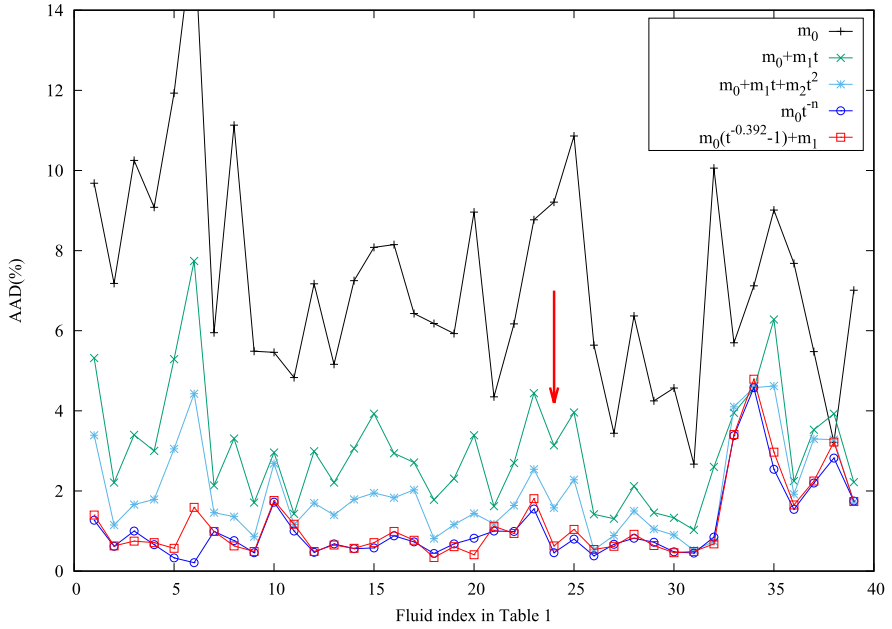


**Fig. 4.** Absolute average deviations (AADs) for all the fluids included in Table 1 when different correlations for the reduced influence parameter are considered. The vertical arrow indicates the position of methyl linoleate.

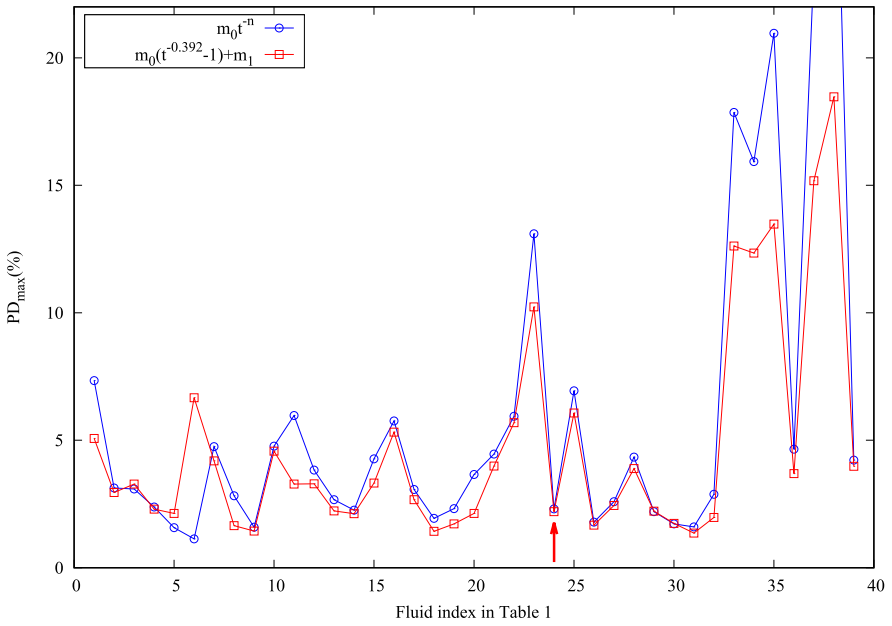


**Fig. 5.** Maximum absolute percentage deviations for the surface tension when the correlations given by Eq. (27) and by Zuo and Stenby, Eq. (17), are used. The vertical arrow line indicates the position of methyl linoleate.

overall absolute deviation (OAAD):

$$\mathrm{OAAD} = \frac{1}{N_{total}} \sum_{i=1}^{N_{total}} |\mathrm{PD}_i|, \tag{33}$$

where $N_{total}$ is the number of points of the whole dataset, and the overall mean deviation (OMD):

**Table 2**
Fitting parameters of Eqs. (17) and (27) for the fluids considered in this work. $m_0$ and $m_1$ are written in $10^{-17}$mol$^{2/3}$.

| | | Eq. (17) | | | | Eq. (27) | | | |
|---|---|---|---|---|---|---|---|---|---|
| Index | Fluid name | $m_0$ | $n$ | AAD | $PD_{max}$ | $m_0$ | $m_1$ | AAD | $PD_{max}$ |
| 1 | 2,2,4-trimethyl-1,3-pentanediol diisobutyrate | 3.677 | 0.366 | 1.27 | 7.34 | 3.580 | 3.601 | 1.40 | 5.07 |
| 2 | 2-ethoxyethyl acetate | 2.869 | 0.402 | 0.62 | 3.13 | 2.927 | 2.882 | 0.63 | 2.95 |
| 3 | 2-ethylhexyl acrylate | 2.711 | 0.521 | 1.00 | 3.09 | 3.931 | 2.669 | 0.75 | 3.28 |
| 4 | di(2-ethylhexyl) terephthalate | 2.996 | 0.442 | 0.66 | 2.38 | 3.558 | 2.983 | 0.71 | 2.30 |
| 5 | di-n-butyl phthalate | 2.980 | 0.446 | 0.33 | 1.57 | 3.674 | 2.941 | 0.57 | 2.13 |
| 6 | dibutyl terephthalate | 2.523 | 0.618 | 0.21 | 1.13 | 5.125 | 2.420 | 1.59 | 6.67 |
| 7 | diethyl phthalate | 3.389 | 0.441 | 0.99 | 4.75 | 4.049 | 3.348 | 0.99 | 4.19 |
| 8 | diethylene glycol monobutyl ether acetate | 1.451 | 0.530 | 0.76 | 2.82 | 2.171 | 1.412 | 0.63 | 1.65 |
| 9 | dimethyl maleate | 3.702 | 0.448 | 0.46 | 1.59 | 4.447 | 3.710 | 0.49 | 1.44 |
| 10 | ethyl acetate | 3.639 | 0.442 | 1.72 | 4.77 | 4.488 | 3.563 | 1.76 | 4.57 |
| 11 | ethyl acrylate | 3.643 | 0.502 | 1.00 | 5.97 | 5.458 | 3.461 | 1.17 | 3.28 |
| 12 | ethyl caprate | 3.747 | 0.428 | 0.47 | 3.83 | 4.325 | 3.698 | 0.49 | 3.29 |
| 13 | ethyl caprylate | 3.341 | 0.461 | 0.68 | 2.67 | 4.253 | 3.292 | 0.65 | 2.23 |
| 14 | ethyl laurate | 3.783 | 0.429 | 0.56 | 2.26 | 4.301 | 3.770 | 0.57 | 2.12 |
| 15 | ethyl myristate | 4.150 | 0.401 | 0.58 | 4.27 | 4.447 | 4.135 | 0.71 | 3.32 |
| 16 | ethyl oleate | 4.117 | 0.412 | 0.88 | 5.76 | 4.460 | 4.140 | 0.99 | 5.32 |
| 17 | ethyl palmitate | 4.577 | 0.386 | 0.73 | 3.07 | 4.617 | 4.580 | 0.77 | 2.67 |
| 18 | ethyl phenyl acetate | 3.488 | 0.471 | 0.44 | 1.94 | 4.370 | 3.487 | 0.34 | 1.43 |
| 19 | ethyl stearate | 4.749 | 0.323 | 0.68 | 2.32 | 3.732 | 4.769 | 0.61 | 1.72 |
| 20 | isopentyl butyrate | 2.810 | 0.671 | 0.82 | 3.66 | 6.019 | 2.662 | 0.41 | 2.13 |
| 21 | methyl caprylate | 3.705 | 0.330 | 1.00 | 4.46 | 2.941 | 3.680 | 1.12 | 3.99 |
| 22 | methyl erucate | 4.009 | 0.303 | 0.99 | 5.94 | 2.904 | 4.042 | 0.94 | 5.69 |
| 23 | methyl formate | 4.000 | 0.357 | 1.55 | 13.10 | 3.097 | 4.138 | 1.81 | 10.23 |
| 24 | methyl linoleate | 2.644 | 0.520 | 0.46 | 2.31 | 3.905 | 2.609 | 0.63 | 2.20 |
| 25 | methyl linolenate | 3.125 | 0.515 | 0.80 | 6.94 | 4.675 | 3.028 | 1.04 | 6.07 |
| 26 | methyl methacrylate | 5.412 | 0.287 | 0.38 | 1.79 | 3.552 | 5.432 | 0.54 | 1.67 |
| 27 | methyl myristate | 4.307 | 0.255 | 0.67 | 2.59 | 2.624 | 4.296 | 0.62 | 2.44 |
| 28 | methyl oleate | 3.855 | 0.423 | 0.82 | 4.34 | 4.287 | 3.878 | 0.92 | 3.89 |
| 29 | methyl palmitate | 4.449 | 0.280 | 0.72 | 2.20 | 2.931 | 4.461 | 0.64 | 2.22 |
| 30 | methyl stearate | 4.620 | 0.347 | 0.48 | 1.72 | 3.954 | 4.626 | 0.46 | 1.74 |
| 31 | n-butyl acrylate | 3.466 | 0.289 | 0.45 | 1.60 | 2.332 | 3.489 | 0.49 | 1.36 |
| 32 | *tert*-butyl methacrylate | 2.795 | 0.469 | 0.85 | 2.88 | 3.535 | 2.767 | 0.68 | 1.97 |
| 33 | tricaprin | 5.764 | 0.268 | 3.38 | 17.86 | 3.968 | 5.776 | 3.41 | 12.62 |
| 34 | tricaprylin | 5.110 | 0.296 | 4.58 | 15.93 | 4.068 | 5.239 | 4.79 | 12.34 |
| 35 | trilaurin | 6.740 | 0.309 | 2.54 | 20.96 | 6.238 | 6.475 | 2.97 | 13.48 |
| 36 | trimyristin | 7.674 | 0.389 | 1.54 | 4.65 | 7.239 | 7.901 | 1.65 | 3.69 |
| 37 | tripalmitin | 9.213 | 0.254 | 2.20 | 23.45 | 6.810 | 9.184 | 2.25 | 15.18 |
| 38 | tristearin | 11.003 | 0.072 | 2.82 | 33.07 | 4.306 | 10.699 | 3.22 | 18.47 |
| 39 | vinyl acetate | 3.612 | 0.464 | 1.75 | 4.22 | 4.726 | 3.567 | 1.74 | 3.98 |

**Table 3**
Absolute Average Deviations (AAD), Mean Deviations (MD) and maximum absolute percentage deviations ($PD_{max}$) obtained for methyl linoleate when the different correlations are taken into account.

| Equation | AAD (%) | MD (%) | $PD_{max}$ (%) |
|---|---|---|---|
| Constant, $m_0$ | 9.21 | −7.15 | 36.33 |
| Eq. (15), $m_0 + m_1 t$ | 3.14 | −0.18 | 13.57 |
| Eq. (16), $m_0 + m_1 t + m_2 t^2$ | 1.58 | −0.04 | 6.17 |
| Eq. (17), $m_0 t^{-n}$ | 0.46 | 0.075 | 2.31 |
| Eq. (27), $m_0(t^{-0.392} - 1) + m_1$ | 0.63 | −0.0065 | 2.20 |

$$\mathrm{OMD} = \frac{1}{N_{total}} \sum_{i=1}^{N_{total}} \mathrm{PD}_i. \tag{34}$$

## 5. Results and discussion

Fig. 2, for methyl linoleate, can be considered as an example of the behavior of the reduced influence parameter $c^*$ versus the reduced temperature $t$ for most fluids. Here, the points are the values obtained when Eq. (10) is applied together with the Peng-Robinson EoS for the 23 surface tension data taken from Refs. [52,58], and the lines are the correlations obtained when minimizing the AAD, Eq. (29).

The shape of the curve in Fig. 2a shows a negative slope with positive curvature and the asymptotic behavior expected at temperatures near the critical point ($t = 0$). Thus, the observed behavior does not follow a constant or linear correlation, and even a

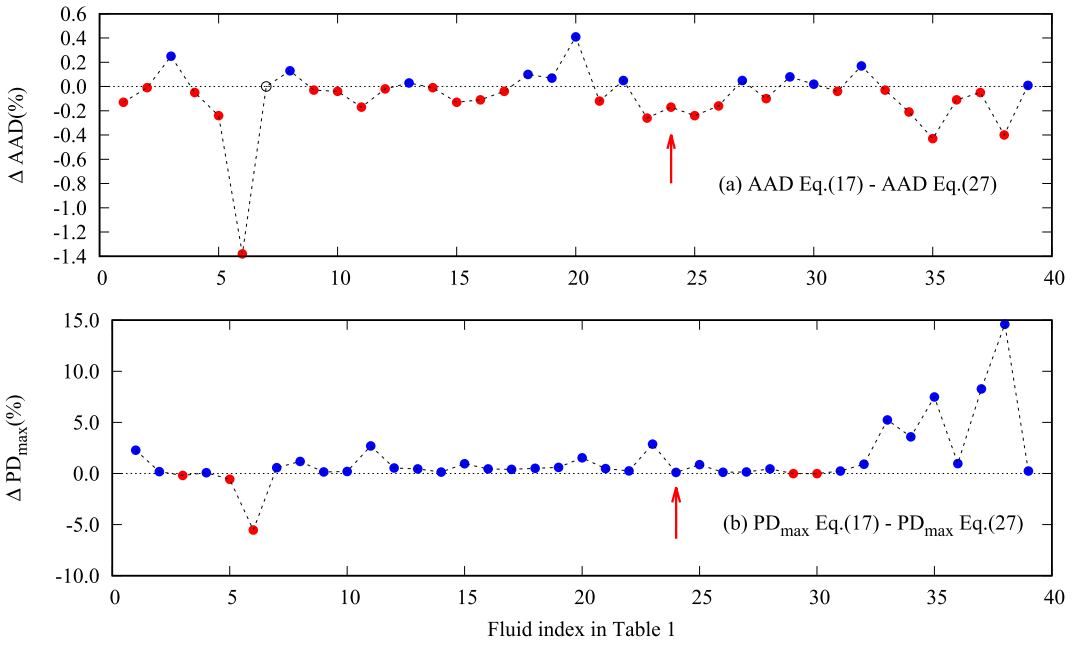


**Fig. 6.** Differences between the AAD (a) and $PD_{max}$ (b) predicted with Eqs. (17) and (27). A positive value indicates that Eq. (27) gives a lower AAD (or $PD_{max}$) than Eq. (17). Positive values are in solid blue, negative solid red, and zero in open circles. The arrow indicates the position of methyl linoleate. (For interpretation of the references to colour in this figure legend, the reader is referred to the Web version of this article.)

**Table 4**
Overall absolute deviations (OAAD) and overall mean deviations (OMD) obtained in the calculation of the surface tension for all the temperature-dependent correlations considered for the reduced influence parameter.

| Equation | OAAD (%) | OMD (%) |
|---|---|---|
| $m_0$ | 6.53 | −3.40 |
| Eq. (15), $m_0 + m_1 t$ | 2.92 | −0.23 |
| Eq. (16), $m_0 + m_1 t + m_2 t^2$ | 2.06 | −0.12 |
| Eq. (17), $m_0 t^{-n}$ | 1.29 | −0.13 |
| Eq. (27), $m_0(t^{-0.392} - 1) + m_1$ | 1.37 | −0.05 |

quadratic polynomial is not an appropriate representation. Nevertheless, when the surface tension is calculated, the high percentage deviations observed in the influence parameter for these correlations are considerably reduced (see in Fig. 3).

The statistical figures of the surface tension for methyl linoleate (Table 3) show that a constant term (one fitting parameter) leads to a very high maximum percentage deviation 36.33% (being around 60% for the influence parameter, as shown in 2b). The linear and quadratic correlations, with the same or one more fitting parameters, respectively, give worse results than those from Zuo and Stenby, Eq. (17), and our proposal, Eq. (27). Only by introducing the appropriate analytical form, as done only in Eqs. (17) and (27), the data with an asymptotic behavior near the critical point are well represented. (Fitting parameters, AAD, and $PD_{max}$, for the constant, linear, and quadratic correlations are compiled in Table S1 in the supplementary material for all the fluids considered).

For methyl linoleate, the $PD_{max}$ of Eqs. (17) and (27), 2.31% and 2.20%, respectively, are due to the disagreement between the surface tension data obtained from different sources ([52,58], respectively) in the low temperature range, and not to the high temperature behavior. In this range, despite the different exponent associated with the asymptotic behavior (0.392 for our proposal, and 0.520 for the Zuo and Stenby correlation), both models agree well with the available data.

Figs. 4 and 5 show the AADs and $PD_{max}$ values obtained with the different models for every ester considered in this work, where the case of methyl linoleate (fluid number 24) is not an exception and represents well the general behavior. The correlations in Eqs. (27) and (17) are, by far, the best choices when low AADs for the surface tension are required.

Table 2 lists the fitting parameters, AADs, and $PDs_{max}$ of the Zuo and Stenby proposal, Eq. (17), and ours, Eq. (27). It can be seen that both correlations yield a $PD_{max}$ higher than 10% for six fluids: methyl formate, tricaprin, tricaprylin, trilaurin, tripalmitin, and tristearin, although all AADs are below 4.8%. The disagreements are due to the different data trends in the low and high-temperature ranges. A high number of data at lower temperatures lead to a parameter set that minimizes the percentage deviations of those data, and the high-temperature range is not well fitted (figures for all the fluids are available as supplementary material).

A graphical comparison between AADs and $PDs_{max}$ obtained by the Zuo and Stenby and Eq. (27) correlations, is done in Fig. 6. Fig. 6a shows that both correlations give almost the same AADs, with the exception of dibutyl terephthalate (fluid number 6 in Tables 1 and 2) where the correlation of Zuo and Stenby yields an AAD 1.38% lower than the given by the correlation here proposed.

Nevertheless, the AAD obtained with our proposal is 1.59%, which can also be considered a low value, similar to the results obtained for other esters.

In relation to the $PD_{max}$, Fig. 6b shows that the behavior of both correlations are similar (being our proposal slightly better), with differences higher than 5% only in five fluids, being tristearin the fluid for which the higher difference is found.

Table 4 shows the overall absolute and mean deviations for the surface tension of the 39 esters obtained by using the five correlations considered here for the influence parameter. It is clear that a constant influence parameter yields very bad results when the temperature range covered is wide, with OAAD = 6.53%, and MD = −3.40%, which indicates under-prediction. Besides, considering that Eq. (15) and Eq. (16) have the same, or one more fitting parameter, it is clear that, in general, Eq. (17) and Eq. (27) should be used instead the linear and quadratic expressions.

The OAAD of 1.37% obtained with our proposal, Eq. (27), is slightly worse than the corresponding one from Zuo and Stenby, Eq. (17), of 1.29%, but it is compensated with a better (closer to zero) overall mean deviation (−0.05%) than the one obtained with Zuo and Stenby's proposal (−0.13%). Despite the similar behavior, the expression proposed here has a more substantial theoretical basis, as the temperature exponent is related to the universal scale law exponent associated with the liquid-vapor phase change near the critical point.

## 6. Conclusions

The behavior of five different analytical expressions for the influence parameter in density gradient theory combined with the Peng-Robinson equation of state is analyzed. When considering the surface tension values for 39 esters, it is found that constant, linear, or quadratic correlations with temperature can only be considered when the range studied is narrow enough.

It is shown that the introduction of an asymptote at the critical temperature in the analytical expression of the influence parameter is necessary to reproduce its behavior at temperatures near the critical one. Two fitting parameters are enough to reproduce the available surface tension data accurately with the appropriate analytical form.

The here-proposed analytical expression, that contains a universal exponent related to the liquid-vapor phase change universal scale law exponent, reproduces the available data with the same accuracy as the other correlation considered where this exponent is not fixed.

## Author agreement statement

We the undersigned declare that this manuscript is original, has not been published before and is not currently being considered for publication elsewhere.

We confirm that the manuscript has been read and approved by all named authors and that there are no other persons who satisfied the criteria for authorship but are not listed.

We further confirm that the order of authors listed in the manuscript has been approved by all of us.

We understand that the Corresponding Author is the sole contact for the Editorial process.

He/she is responsible for communicating with the other authors about progress, submissions of revisions and final approval of proofs.

## Declaration of competing interest

The authors declare that they have no known competing financial interests or personal relationships that could have appeared to influence the work reported in this paper.

## Acknowledgments

Authors thank the financial support received from the "Junta de Extremadura" and European Regional Development Fund (ERDF A way of making Europe) through project GR21012, and from the "Ministerio de Ciencia e Innovación" and "Agencia Estatal de Investigación" (http://doi.org/10.13039/501100011033) of the Spanish Government, and FEDER through project PGC2018-098418-B-I00.

## Appendix A. Supplementary data

Supplementary data to this article can be found online at https://doi.org/10.1016/j.csite.2022.102193.

## Appendix

It is said in the introduction that the ideal isochoric caloric capacity does not influence the determination of the influence parameter. The first step in the demonstration is to operate in the argument of the square root (*ASQR*) of Eq. (1). Thus:

$$ASQR = f_0 - \rho\left(\frac{\partial f_0}{\partial \rho}\right)_T^0 + p^0 = \rho f - \rho\left(\frac{\partial(\rho f)}{\partial \rho}\right)_T^0 + p^0 = \rho(f - f^0) - \rho\rho^0\left(\frac{\partial f}{\partial \rho}\right)_T^0 + p^0. \tag{35}$$

Taking into account the relation between pressure and Helmholtz energy:

$$p = \rho^2 \left(\frac{\partial f}{\partial \rho}\right)_T, \tag{36}$$

the saturation pressure is written as:

$$p^0 = (\rho^0)^2 \left(\frac{\partial f}{\partial \rho}\right)_T^0. \tag{37}$$

The last part on the right-hand side of Eq. (35) can be written as:

$$-\rho\rho^0 \left(\frac{\partial f}{\partial \rho}\right)_T^0 + p^0 = -\frac{\rho}{\rho^0}(\rho^0)^2 \left(\frac{\partial f}{\partial \rho}\right)_T^0 + p^0 = p^0\left(1 - \frac{\rho}{\rho^0}\right), \tag{38}$$

that inserted in (35) results in:

$$ASQR = \rho(f - f^0) + p^0\left(1 - \frac{\rho}{\rho^0}\right). \tag{39}$$

By splitting the Helmholtz energy into the residual and ideal parts, the contribution $f - f^0$ in Eq. (39) is:

$$f - f^0 = f^r - (f^r)^0 + f^\circ - f^\circ 0.$$

Considering that the evaluation of *ASQR* is done at constant temperature, the difference $f^\circ - f^\circ 0$ can be written using Eq. (5) as

$$f^\circ - f^\circ 0 = RT\log(\rho / \rho^0). \tag{40}$$

Then, the argument of the integral can be written as:

$$ASQR = \rho[f^r - (f^r)^0 + RT\ln(\rho / \rho^0)] + p^0\left(1 - \frac{\rho}{\rho^0}\right), \tag{41}$$

where there is no dependency on $c_p^\circ$.

## References


[1] L. Lomba, B. Giner, I. Bandrés, C. Lafuente, M.R. Pino, Physicochemical properties of green solvents derived from biomass, Green Chem. 13 (8) (2011) 2062–2070.
[2] L.F. Ramírez-Verduzco, Models for predicting the surface tension of biodiesel and methyl esters, Renew. Sustain. Energy Rev. 41 (2015) 202–216.
[3] T. Wallek, K. Knöbelreiter, J. Rarey, Estimation of pure-component properties of biodiesel-related components: fatty acid ethyl esters, Ind. Eng. Chem. Res. 57 (9) (2018) 3382–3396.
[4] D.B. Macleod, On a relation between surface tension and density, Trans. Faraday Soc. 19 (July) (1923) 38–41.
[5] Y.-X. Zuo, E.H. Stenby, Corresponding-states and parachor models for the calculation of interfacial tensions, Can. J. Chem. Eng. 75 (6) (1997) 1130–1137.
[6] G.J. Gloor, G. Jackson, F.J. Blas, E.M. del Río, E. de Miguel, An accurate density functional theory for the vapor-liquid interface of associating chain molecules based on the statistical associating fluid theory for potentials of variable range, J. Chem. Phys. 121 (24) (2004) 12740–12759.
[7] M.B. Oliveira, J.A.P. Coutinho, A.J. Queimada, Surface tensions of esters from a combination of the gradient theory with the CPA EoS, Fluid Phase Equil. 303 (1) (2011) 56–61.
[8] B.S. Carey, L.E. Scriven, H.T. Davis, Semiempirical theory of surface tensions of pure normal alkanes and alcohols, AIChE J. 24 (6) (1978) 1076–1080.
[9] Y.-X. Zuo, E.H. Stenby, Calculation of interfacial tensions with gradient theory, Fluid Phase Equil. 132 (1–2) (1997) 139–158.
[10] C. Miqueu, B. Mendiboure, A. Graciaa, J. Lachaise, Modelling of the surface tension of pure components with the gradient theory of fluid interfaces: a simple and accurate expression for the influence parameters, Fluid Phase Equil. 207 (1–2) (2003) 225–246.
[11] A. Hernández, Interfacial behavior prediction of alcohol+ glycerol mixtures using gradient theory, Chem. Phys. 534 (2020), 110747.
[12] A. Hernández, S. Khosharay, Investigation on the surface tension and viscosity of (dimethylsulfoxide+ alcohol) mixtures by using gradient theory and Eyring's rate theory, Int. J. Thermophys. 41 (11) (2020) 1–22.
[13] A. Hernández, D. Zabala, Modeling of the interfacial behavior of carbon dioxide+ methyl myristate, carbon dioxide+ palmitate, and carbon dioxide+ methyl myristate+ methyl palmitate mixtures using CPA-EOS and gradient theory, Int. J. Thermophys. 42 (3) (2021) 1–21.
[14] F. Biglar, A. Hernández, S. Khosharay, Modeling of the interfacial behavior of $CO_2$ + $H_2O$ and $H_2S$ + $H_2O$ with CPA EOS and gradient theory, Int. J. Thermophys. 42 (7) (2021) 1–19.
[15] J.W. Cahn, J.E. Hilliard, Free energy of a nonuniform system. I. Interfacial free energy, J. Chem. Phys. 28 (2) (1958) 258–267.
[16] J.M. Garrido, A. Mejía, M.M. Piñeiro, F.J. Blas, E.A. Müller, Interfacial tensions of industrial fluids from a molecular-based square gradient theory, AIChE J. 62 (5) (2016) 1781–1794.
[17] R. Span, Multiparameter Equations of State: an Accurate Source of Thermodynamic Property Data, Springer-Verlag, 2001.
[18] A.J.M. Yang, P.D. Fleming III, J.H. Gibbs, Molecular theory of surface tension, J. Chem. Phys. 64 (9) (1976) 3732–3747.
[19] X. Liang, M.L. Michelsen, G.M. Kontogeorgis, A density gradient theory based method for surface tension calculations, Fluid Phase Equil. 428 (2016) 153–163.
[20] J.M. Garrido, I. Polishuk, Toward development of a universal CP-PC-SAFT-based modeling framework for predicting thermophysical properties at reservoir conditions: inclusion of surface tensions, Ind. Eng. Chem. Res. 57 (26) (2018) 8819–8831.
[21] Y.T.F. Chow, D.K. Eriksen, A. Galindo, A.J. Haslam, G. Jackson, G.C. Maitland, J.P.M. Trusler, Interfacial tensions of systems comprising water, carbon dioxide and diluent gases at high pressures: experimental measurements and modelling with SAFT-VR Mie and square-gradient theory, Fluid Phase Equil. 407 (2016) 159–176.
[22] P.M.W. Cornelisse, C.J. Peters, J. de Swaan Arons, Application of the Peng-Robinson equation of state to calculate interfacial tensions and profiles at vapour-liquid interfaces, Fluid Phase Equil. 82 (1993) 119–129.
[23] P.M. Larsen, B. Maribo-Mogensen, G.M. Kontogeorgis, A collocation method for surface tension calculations with the density gradient theory, Fluid Phase Equil. 408 (2016) 170–179.

[24] J.H. Pérez-López, L.J. González-Ortiz, M.A. Leiva, J.E. Puig, Estimation of surface tension of pure fluids using the gradient theory, AIChE J. 38 (5) (1992) 753–760.
[25] Y.-X. Zuo, E.H. Stenby, A linear gradient theory model for calculating interfacial tensions of mixtures, J. Colloid Interface Sci. 182 (1) (1996) 126–132.
[26] A. Mejía, H. Segura, J. Wisniak, I. Polishuk, Correlation and prediction of interface tension for fluid mixtures: an approach based on cubic equations of state with the Wong-Sandler mixing rule, J. Phase Equilibria Diffus. 26 (3) (2005) 215–224.
[27] A. Mejía, H. Segura, L.F. Vega, J. Wisniak, Simultaneous prediction of interfacial tension and phase equilibria in binary mixtures: an approach based on cubic equations of state with improved mixing rules, Fluid Phase Equil. 227 (2) (2005) 225–238.
[28] E.A. Müller, A. Mejía, Interfacial properties of selected binary mixtures containing n-alkanes, Fluid Phase Equil. 282 (2) (2009) 68–81.
[29] M.B. Oliveira, S.V.D. Freitas, F. Llovell, L.F. Vega, João A.P. Coutinho, Development of simple and transferable molecular models for biodiesel production with the soft-SAFT equation of state, Chem. Eng. Res. Des. 92 (12) (2014) 2898–2911.
[30] B. Breure, C.J. Peters, Modeling of the surface tension of pure components and mixtures using the density gradient theory combined with a theoretically derived influence parameter correlation, Fluid Phase Equil. 334 (2012) 189–196.
[31] N. Haarmann, A. Reinhardt, A. Danzer, G. Sadowski, S. Enders, Modeling of interfacial tensions of long-chain molecules and related mixtures using perturbed chain-statistical associating fluid theory and the density gradient theory, J. Chem. Eng. Data 65 (3) (2019) 1005–1018.
[32] Jean-Noël Jaubert, Romain Privat, Thermodynamic Models for Chemical Processes, ISTE Press, 2021.
[33] G.M. Kontogeorgis, G.K. Folas, Thermodynamic Models for Industrial Applications: from Classical and Advanced Mixing Rules to Association Theories, John Wiley & Sons, 2009.
[34] C. Tsonopoulos, J.L. Heidman, High-pressure vapor-liquid equilibria with cubic equations of state, Fluid Phase Equil. 29 (1986) 391–414.
[35] A. Hernández, Modeling vapor-liquid equilibria and surface tension of carboxylic acids + water mixtures using Peng-Robinson equation of state and gradient theory, Int. J. Thermophys. 42 (13) (2021) 1–27.
[36] A. Hernández, R. Tahery, Modeling of phase equilibria and surface tension for n,n-dimethylcyclohexylamine + alcohol mixtures at different temperatures, Int. J. Thermophys. 42 (67) (2021) 1–27.
[37] A. Hernández, R. Tahery, Modeling of surface tension and phase equilibria for water+ amine mixtures from (298.15 to 323.15) K using different thermodynamic models, J. Solut. Chem. (2022) 1–27.
[38] D.-Y. Peng, D.B. Robinson, A new two-constant equation of state, Ind. Eng. Chem. Fundam. 15 (1) (1976) 59–64.
[39] J.S. Lopez-Echeverry, S. Reif-Acherman, E. Araujo-Lopez, Peng-Robinson equation of state: 40 years through cubics, Fluid Phase Equil. 447 (2017) 39–71.
[40] W.H. Press, S.A. Teukolsky, W.T. Vetterling, B.P. Flannery, Numerical Recipes 3rd Edition: the Art of Scientific Computing, Cambridge University Press, 2007.
[41] P.M.W. Cornelisse, *The Gradient Theory Applied, Simultaneous Modelling Of Interfacial Tension And Phase Behaviour*. PhD Thesis, Technische Universiteit Delft, 1997.
[42] A. Mulero, I. Cachadiña, M.I. Parra, Recommended correlations for the surface tension of common fluids, J. Phys. Chem. Ref. Data 41 (4) (2012), 043105.
[43] A. Mulero, I. Cachadiña, Recommended correlations for the surface tension of several fluids included in the REFPROP program, J. Phys. Chem. Ref. Data 43 (2) (2014), 023104.
[44] A. Mulero, I. Cachadiña, E.L. Sanjuán, Recommended correlations for the surface tension of aliphatic, carboxylic, and polyfunctional organic acids, J. Phys. Chem. Ref. Data 45 (3) (2016), 033105.
[45] A. Mulero, I. Cachadiña, D. Bautista, Recommended correlations for the surface tension of *n*-alkanes, J. Phys. Chem. Ref. Data 50 (2021), 023104.
[46] A. Mulero, I. Cachadiña, A. Vegas, Recommended correlations for the surface tension of 80 esters, J. Phys. Chem. Ref. Data 50 (2021), 033106.
[47] A. Mulero, I. Cachadiña, A. Vegas, Recommended correlations for the surface tension of aromatic, polyfunctional and glyceride esters, J. Phys. Chem. Ref. Data 51 (2022), 023102, https://doi.org/10.1063/5.0092546.
[48] O.R. Quayle, The parachors of organic compounds. an interpretation and catalogue, Chem. Rev. 53 (3) (1953) 439–589.
[49] F. Gharagheizi, A. Eslamimanesh, A.H. Mohammadi, D. Richon, Determination of parachor of various compounds using an artificial neural network- group contribution method, Ind. Eng. Chem. Res. 50 (9) (2011) 5815–5823.
[50] J.V. Sengers, J.M.H.L. Sengers, Thermodynamic behavior of fluids near the critical point, Annu. Rev. Phys. Chem. 37 (1) (1986) 189–222.
[51] I. Brovchenko, A. Oleinikova, Interfacial and Confined Water, Elsevier, 2008.
[52] R.L. Rowley, W.V. Wilding, J.L. Oscarson, T.A. Knotts, N.F. Giles, DIPPR®Data Compilation Of Pure Chemical Properties, AIChE, New York, NY, 2020.
[53] Detherm, Thermophysical Properties of Pure Substances & Mixtures, DECHEMA, Gesellschaft für Chemische Techink und Biotechnologie e.V., 2018, 2018.
[54] Ch Wohlfarth, B. Wohlfarth, Surface Tension of Pure Liquids and Binary Liquid Mixtures, Springer, 1997.
[55] Ch Wohlfarth, Surface Tension of Pure Liquids and Binary Liquid Mixtures, Supplement to IV/16, Springer, 2008.
[56] C. Wohlfarth, M. Lechner, Surface Tension of Pure Liquids and Binary Liquid Mixtures: Supplement to, ume IV/24, Springer, 2016.
[57] S. Sugden, Vi.—the variation of surface tension with temperature and some related functions, J. Chem. Soc. Trans. 125 (1924) 32–41.
[58] C.E. Ejim, B.A. Fleck, A. Amirfazli, Analytical study for atomization of biodiesels and their blends in a typical injector: surface tension and viscosity effects, Fuel 86 (10–11) (2007) 1534–1544.
[59] V. Goussard, F. Duprat, V. Gerbaud, J.-L. Ploix, G. Dreyfus, V. Nardello-Rataj, J.-M. Aubry, Predicting the surface tension of liquids: comparison of four modeling approaches and application to cosmetic oils, J. Chem. Inf. Model. 57 (12) (2017) 2986–2995.
[60] R. Naef, W.E. Acree, Calculation of the surface tension of ordinary organic and ionic liquids by means of a generally applicable computer algorithm based on the group-additivity method, Molecules 23 (5) (2018) 1224.
[61] A. Kalantarian, S.M.I. Saad, A.W. Neumann, Accuracy of surface tension measurement from drop shapes: the role of image analysis, Adv. Colloid Interface Sci. 199 (2013) 15–22.
[62] S.M.I. Saad, Z. Policova, A.W. Neumann, Design and accuracy of pendant drop methods for surface tension measurement, Colloids Surf. A Physicochem. Eng. Asp. 384 (1–3) (2011) 442–452.
[63] J.N. Stuecker, J. Cesarano III, E.L. Corral, K.A. Shollenberger, R. Allen Roach, J.R. Torczynski, E.V. Thomas, D.J. Van Ornum, Filling Source Feedthrus with Alumina/molybdenum Cnd50 Cermet: Experimental, Theoretical, and Computational Approaches, 2001.
[64] D.R. Lide, CRC Handbook of Chemistry and Physics, vol. 86, CRC press, 2005.
[65] S. Ahadian, S. Moradian, M. Mohseni, T.M. Amani, F. Sharif, Determination of surface tension and viscosity of liquids by the aid of the capillary rise procedure using artificial neural network (ANN), Iran. J. Chem. Chem. Eng. (Int. Engl. Ed.) (2008).
[66] E.J. Delgado, G.A. Díaz, A molecular structure based model for predicting surface tension of organic compounds, SAR QSAR Environ. Res. 17 (5) (2006) 483–496.
[67] J.J. Jasper, The surface tension of pure liquid compounds, J. Phys. Chem. Ref. Data 1 (4) (1972) 841–1010.
[68] J. Lielmezs, T.A. Herrick, New surface tension correlation for liquids, Chem. Eng. J. 32 (3) (1986) 165–169.
[69] J. de los S. López-Lázaro, G.A. Iglesias-Silva, A. Estrada-Baltazar, J. Barajas-Fernández, Density and surface tension of binary mixtures of 2, 2, 4-trimethylpentane+ n-heptane, 2, 2, 4-trimethylpentane+ n-octane, ethyl acetate+ benzene, and butanenitrile+ benzene from (293.15 to 323.15) K, J. Chem. Eng. Data 60 (6) (2015) 1823–1834.
[70] S.R.S. Sastri, K.K. Rao, A simple method to predict surface tension of organic liquids, Chem. Eng. J. Biochem. Eng. J. 59 (2) (1995) 181–186.
[71] M. Singh, Survismeter for simultaneous viscosity and surface tension study for molecular interactions, Surf. Interface Anal.: An International Journal devoted to the development and application of techniques for the analysis of surfaces, interfaces and thin films 40 (1) (2008) 15–21.
[72] S. Werth, M. Horsch, H. Hasse, Molecular simulation of the surface tension of 33 multi-site models for real fluids, J. Mol. Liq. 235 (2017) 126–134.
[73] L. Lomba, B. Giner, C. Lafuente, S. Martín, H. Artigas, Thermophysical properties of three compounds from the acrylate family, J. Chem. Eng. Data 58 (5) (2013) 1193–1202.
[74] C.A.W. Allen, K.C. Watts, R.G. Ackman, Predicting the surface tension of biodiesel fuels from their fatty acid composition, JAOCS (J. Am. Oil Chem. Soc.) 76 (3) (1999) 317–323.

[75] C.A. Díaz-Tovar, R. Gani, B. Sarup, Computer-aided Modeling of Lipid Processing Technology, PhD thesis, English, 2011.
[76] G. Zhao, Z. Yuan, J. Yin, S. Ma, Thermophysical properties of fatty acid methyl and ethyl esters, J. Chem. Therm. 134 (2019) 195–212.
[77] J.K. Spelt, D.R. Absolom, A.W. Neumann, Solid surface tension: the interpretation of contact angles by the equation of state approach and the theory of surface tension components, Langmuir 2 (5) (1986) 620–625.
[78] J.A. Dean, Lange's Handbook of Chemistry, fourteenth ed., 1992.
[79] D. Swern, Physical properties of fats and fatty acids, in: Bailey's Industrial Oil and Fat Products", John Wiley and Sons, Inc., New York, NY, 1979.
[80] D. Hopfe, Thermophysical Data of Pure Substances, Data Compilation of FIZ CHEMIE, Germany, 1990, p. 20.
[81] I. del Pozo, M. Cartes, F. Llovell, A. Mejía, Densities and interfacial tensions for fatty acid methyl esters (from methyl formate to methyl heptanoate)+ water demixed mixtures at atmospheric pressure conditions, J. Chem. Therm. 121 (2018) 121–128.
[82] M.H. Ghatee, L. Pakdel, Surface tension regularity of non-polar, polar, and weak electrolyte liquid hydrocarbons, Fluid Phase Equil. 234 (1–2) (2005) 101–107.
[83] I.E. Maloka, E.T. Hashim, Estimation of the surface tension of a pure liquid, Petrol. Sci. Technol. 22 (11–12) (2004) 1527–1534.
[84] R.J. Hamilton, Structure and general properties of mineral and vegetable oils used as spray adjuvants, Pestic. Sci. 37 (2) (1993) 141–146.
[85] K.M. Doll, B.R. Moser, S.Z. Erhan, Surface tension studies of alkyl esters and epoxidized alkyl esters relevant to oleochemically based fuel additives, Energy Fuels 21 (5) (2007) 3044–3048.
[86] B. Hajra, M. Kumar, A.K. Pathak, C. Guria, Surface tension and rheological behavior of sal oil methyl ester biodiesel and its blend with petrodiesel fuel, Fuel 166 (2016) 130–142.
[87] R.B. Joglekar, H.E. Watson, The physical properties of pure triglycerides, J. Phys. Chem. Ref. Data 47 (1928) 365–368.
[88] L.D.A. Chumpitaz, L.F. Coutinho, A.J.A. Meirelles, Surface tension of fatty acids and triglycerides, JAOCS (J. Am. Oil Chem. Soc.) 76 (3) (1999) 379–382.
[89] M.-C. Michalski, B.J.V. Saramago, Static and dynamic wetting behavior of triglycerides on solid surfaces, J. Colloid Interface Sci. 227 (2) (2000) 380–389.
[90] S.N. Sahasrabudhe, V. Rodriguez-Martinez, M. O'Meara, B.E. Farkas, Density, viscosity, and surface tension of five vegetable oils at elevated temperatures: measurement and modeling, Int. J. Food Prop. 20 (sup2) (2017) 1965–1981.
[91] A.T. Tyowua, J.M. Mooney, B.P. Binks, Janus liquid marbles containing both oil and water stabilised by silica or sericite particles, Colloids Surf. A Physicochem. Eng. Asp. 560 (2019) 288–297.